557354

Sandia National Laboratories

Operated for the U.S. Department of Energy by the
**Sandia Corporation**

Defense Waste Management Programs
4100 National Parks Highway
Carlsbad, New Mexico 88220

*date:* April 30, 2012

*to:* WIPP Records Center

*from:* Courtney G. Herrick (6211)

*technical review:* Dwayne Kicker (6211)

*QA review:* Shelly Nielsen (6210)

*management review:* Janis Trone (6211)

*subject:* JAS3D Calculations Performed in Support of the PCS-2012 PA Parameters Selections

Calculations performed using Sandia National Laboratories' structural code JAS3D to model panel closures made of 100 ft of run-of-mine salt in the air intake drift of a panel made use of the volumetric creep model. All other aspects of the underground modeling were made in accord with the well-established boundary and loading conditions and stratigraphy used to generate the porosity surface used in Performance Assessment (PA). The modeling results for initial porosities of the run-of-mine salt of 33, 25, 20, and 15% were used previously to answer questions from the U.S. Environmental Protection Agency (EPA) dated December 22, 2011 concerning PC3R PA (DOE 2012). These porosities correspond to initial fractional densities of 67, 75, 80, and 85% of intact salt, respectively. The volumetric model, input parameters, and run control information were briefly described in a memo by Herrick (2012), however a complete model of the underground was not provided and no results were presented. This memorandum presents an expansion of the earlier memo, reviews the modeling methodology, and includes additional results for initial porosities of 35 and 30%, or initial fractional densities of 65 and 70%, respectively. The collective data from the JAS3D analyses are used in to support the parameter selections made in Camphouse et al. (2012) for the PCS-2012 PA.

## 1 Underground Modeling

The underground panels are assumed to be mined at the original design depth of 655 m in the Salado bedded salt formation of southeastern New Mexico. That means that the 2.43 m elevation difference between those panels excavated at the original design horizon and those excavated at the raised level where the back is coincident with Clay Seam G is neglected. In addition, the panel closure model is developed based on the air intake drift of the panel. Being wider (20 ft, 6.10 m) and taller (13 ft, 3.96 m) than the air exhaust drift (14 ft, 4.27 m wide by 12 ft, 3.66 m high), the intake drift is expected to undergo greater deformation.

WIPP:1.2.5:PA:QA-L:554612

The simplified underground stratigraphic model used in geomechanical numerical analyses since the CCA (Butcher 1997, Stone 1997b, Park and Holland 2007) was modified to include the panel intake drift and the distance between adjacent panels (Figure 1). Other than those two changes, the mesh is changed as little as possible from the original mesh used by Stone (1997b) to minimize possible errors introduced by the changes.

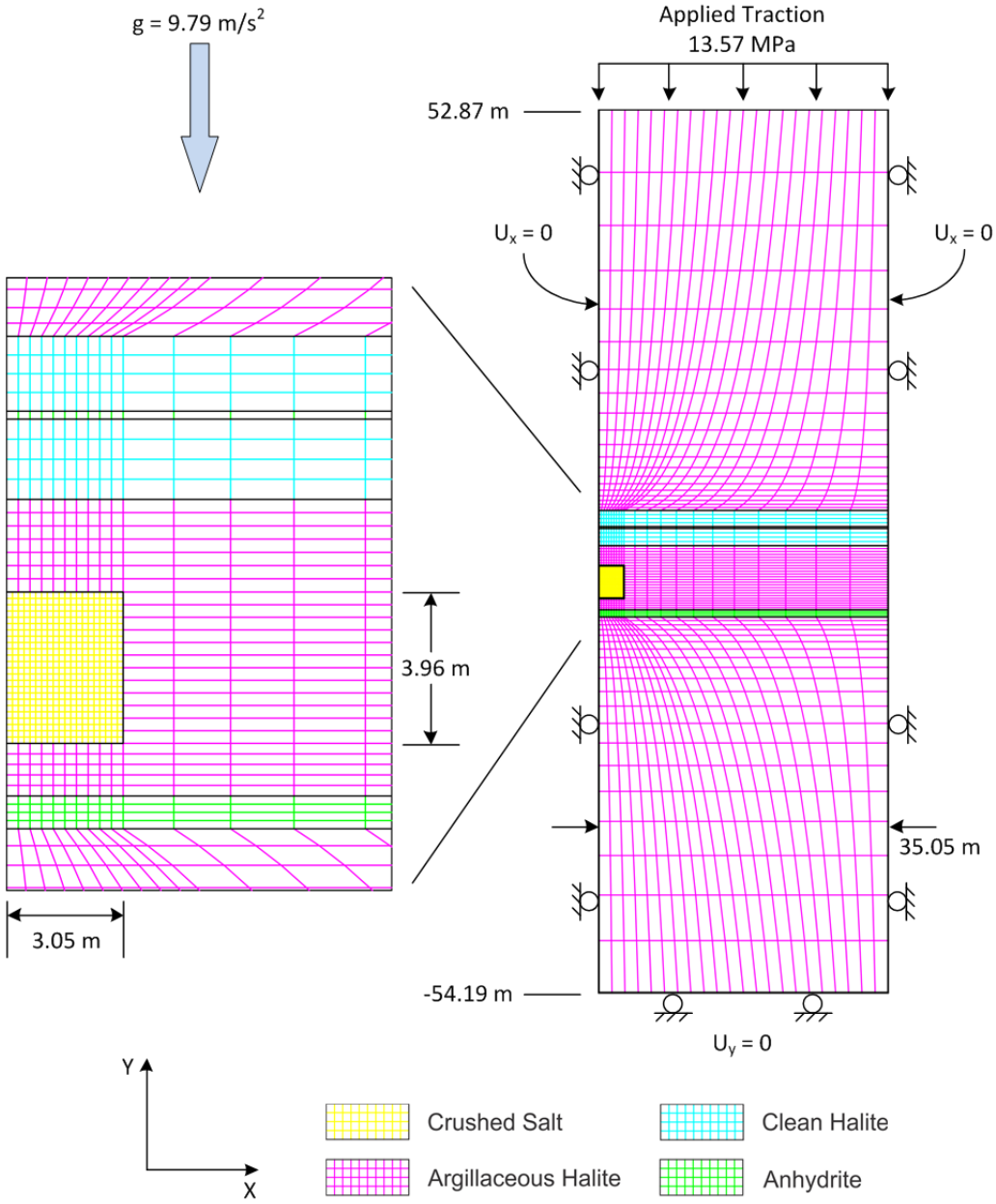


Figure 1. Simplified underground stratigraphic, half symmetry model and boundary conditions used in the JAS3D modeling of crushed salt panel closures.

In order to be used in JAS3D, the model had to be made 3D by adding a depth of 0.5 m. Even though it is a 3D model, a plane strain condition is assumed in the lengthwise direction of the panel closure. As shown in the verification and validation plan / validation document for JAS3D (WIPP PA 2009), modifying the simplified underground mesh to 3D has very little effect on identical underground analyses made for porosity surface calculations. The plane strain assumption for the crushed salt panel closure was shown to be valid based on a simplified 3D analysis of a model panel closure subjected to a constant stress loading condition (DOE 2012).

A plane of symmetry through the center of the panel closure is used to limit the number of elements in the mesh by having to discretize only half of the model, a half symmetry model. This is accomplished by a no horizontal displacement boundary condition imposed on the left boundary of the mesh in Figure 1. The horizontal width of the model corresponds to half the distance between the drifts of adjacent panels, which is 230 ft (70.10 m). Use of another symmetry boundary condition on the right side of the mesh takes into account the influence an identical drift in an adjacent panel. On the top of the model is a traction boundary condition equivalent to the vertical in situ stress at that elevation. On the bottom of the model is a no displacement boundary condition in the vertical direction.

The drift where the panel closure will be is initially completely filled with run-of-mine salt. This salt is modeled using the volumetric creep model for crushed salt. Contact surfaces are invoked between the crushed salt of the panel closure and the intact salt surrounding the drift so that the materials can deform independently and separate if necessary. In addition, the air pressure in the drift is assumed to be at one atmosphere and obey the ideal gas law.

## 2 The Crushed Salt Constitutive Model

The run-of-mine salt making up the panel closure is modeled using the volumetric creep model in JAS3D. The volumetric creep model is based on the work of Sjaardema and Krieg (1987). They developed their model based on the hydrostatic consolidation tests of crushed salt by Holcomb and Shields (1987). The following description of the model is based on those found in Stone (1997a) who describes how the model was implemented into various Sandia structural mechanics codes. The model was used because of its similarity to the crushed salt model in FLAC3D (Itasca, 2003), used by RockSol Consulting Group, Inc. for the panel closure design document.

The total strain rate is decomposed into volumetric and deviatoric parts. Because intact salt creeps deviatorically when subjected to a deviatoric stress condition, crushed salt should logically be expected to also creep deviatorically. This expectation becomes more reasonable as the density increases and the crushed salt approaches an intact condition. The deviatoric salt creep model used in the volumetric creep model is based on the power-law creep model. The volumetric creep model is formulated such that the material response of the consolidated crushed salt becomes identical to that of the intact material as the density of the crushed salt approaches that of intact salt. The FLAC/FLAC3D crushed salt model used by RockSol differs from the Sandia model in that it appears to include primary creep as well as secondary creep in its implementation (Itasca, 2003). The solution technique is also different.

The bulk, $K$, and shear, $G$, elastic moduli were found from Holcomb and Shields tests to depend on the density, $\rho$, of the material through relationships of the form

$$K = K_0 \exp\left(K_1 \rho\right) \tag{1}$$

$$G = G_0 \exp\left(G_1 \rho\right) \tag{2}$$

where $K_0$, $K_1$, $G_0$, and $G_1$ are material constants.

The power-law creep model is cast as a conventional power-law secondary creep model of the form

$$\dot{\varepsilon} = A\bar{\sigma}^m \exp\left(\frac{-Q}{R\Theta}\right) \tag{3}$$

where $\bar{\sigma}$ is the effective deviatoric stress, $A$ and $m$ are material constants, $\Theta$ is the absolute temperature, $R$ is the universal gas constant, and $Q$ is the activation energy. Using forward Euler integration and a creep strain rate for von Mises flow, the expression for the deviatoric stress rate is given by:

$$\dot{S}_{ij}^n = 2G\left(\dot{\varepsilon}_{ij} - \frac{3}{2}\exp\left(\frac{-Q}{R\Theta}\right)\bar{\sigma}^{m-1}S_{ij}^n\right) \tag{4}$$

The volumetric creep model is developed by extension of a one dimensional problem into three dimensions. A uniaxially compressed porous crushed salt sample is envisioned as being composed of cylinders of salt, each of which has intact salt secondary creep behavior separated by areas of open space. The local stress acting on the salt cylinders is stated in terms of the average stress on the porous sample. The cross-sectional area of the porous sample is expressed in terms of the net cross-sectional area of the salt cylinders. The final resulting continuum model for the rate of the deviatoric stress of the crushed salt is given as:

$$\dot{S}_{ij}^n = 2G(\rho)\left(\dot{\varepsilon}_{ij} - \frac{3}{2}A\left(\frac{\rho_\infty}{\rho}\right)^m \exp\left(\frac{-Q}{R\Theta}\right)\bar{\sigma}^{m-1}S_{ij}^n\right) \tag{5}$$

where the constants $A$, $Q$, $m$, and $\rho_\infty$ refer to values for the intact salt, $\rho$ is the density.

The volumetric part of the model is divided into elastic and inelastic parts as

$$d_{kk} = \frac{\dot{p}}{K\left(\rho\right)} + d_{kk}^c \tag{6}$$

where $d_{kk}$ is the volumetric strain rate, $\dot{p} = \frac{\dot{\sigma}_{kk}}{3}$ is the rate of change of the pressure, $d_{kk}^{c}$ is the volumetric creep strain rate, and $K(\rho)$ is the density-dependent bulk modulus.

Laboratory consolidation tests have shown that the crushed salt volumetric creep rate can be fit by an expression of the form

$$d_{kk}^{c} = \frac{1}{\rho} B_0 \left[ e^{B_1 p} - 1 \right] e^{A\rho} \tag{7}$$

where $B_0$, $B_1$, and $A$ are material constants. The density is computed from the relationship

$$\rho = \rho_0 \exp\left( \int_{t_0}^{t} d_{kk} dt \right) \tag{8}$$

where $\rho_0$ is the density at time $t_0$.

Equation (6) is solved for $\dot{p}$ and combined with the definition of the volumetric creep strain rate, Eq. (7), to yield

$$\dot{p} = K(\rho) \left[ d_{kk} - \frac{1}{\rho} B_0 \left( e^{B_1 p} - 1 \right) e^{A\rho} \right] \tag{9}$$

which is the expression that is integrated.

### *2.1 Input Parameters for the Crushed Salt Model*

The input parameters used in the volumetric creep model and their sources are given in Table 1. The initial densities, $\rho_0$, corresponding to fractional densities of 65, 67, 70, 75, 80, and 85%, are 1404, 1440, 1512, 1620, 1728, and 1836 kg/m$^3$. These represent, in order, initial porosities of 35, 33, 30, 25, 20, and 15%.

Table 1. Input parameters used for the volumetric creep model panel closure.

| Parameter | Value | Units | Source |
|---|---|---|---|
| $2G_0$ | 2.12e+04 | Pa | Sjaardema and Krieg (1987), p. 59 |
| $K_0$ | 1.76e+04 | Pa | Sjaardema and Krieg (1987), p. 59 |
| D | 5.79e-36 | $1/(Pa^n \cdot s)$ | Krieg (1984), p. 18 |
| n | 4.9 | — | Krieg (1984), p. 18 |
| Q/RT | 20.1422 | — | Krieg (1984), p. 18 |
| $G_1$ | 6.53e-03 | $m^3/kg$ | Sjaardema and Krieg (1987), p. 59 |
| $K_1$ | 6.53e-03 | $m^3/kg$ | Sjaardema and Krieg (1987), p. 59 |
| $B_0$ | 1.30e+08 | $kg/(m^3 \cdot s)$ | Sjaardema and Krieg (1987), pp. 14-15 |
| $B_1$ | 8.20e-07 | 1/Pa | Sjaardema and Krieg (1987), pp. 14-15 |
| A | -1.73e-02 | $m^3/kg$ | Sjaardema and Krieg (1987), p. 14 |
| $\rho_\infty$ | 2160 | $kg/m^3$ | Krieg (1984), p. 14; Brodsky (1994), p. 2 |
| $\rho_0$ | 1404 * | $kg/m^3$ | Initial fractional density of 65% of intact salt |

* The value $\rho_0$ = 1404 $kg/m^3$ is for an initial fractional density of 65% intact, which corresponds to a porosity of 35%. Initial density values at time t=0 vary depending on the predetermined porosity value being analyzed. The six initial porosities used were 15, 20, 25, 30, 33, and 35% (or fractional densities 85, 80, 75, 70, 67, and 65%, respectively).

## 3 Intact Salt Constitutive Model

A combined transient-secondary creep constitutive model for rock salt known as the multi-mechanism deformation (M-D) model proposed by Munson and Dawson (1979, 1982, 1984) and extended by Munson et al. (1989), was used for the clean and argillaceous salt. The model is decomposed into an elastic volumetric part and a deviatoric part.

The elastic volumetric part is defined by

$$\varepsilon_{kk} = \frac{\sigma_{kk}}{3K} \tag{10}$$

where, $\varepsilon_{kk}$ = the total strain components
$\sigma_{kk}$ = the total stress components
$K$ = the elastic bulk modulus

The deviatoric part defined by

$$\dot{s}_{ij} = 2G\left(\dot{e}_{ij} - F\dot{\varepsilon}_s\left[\frac{\cos 2\theta}{\sqrt{J_2}\cos 3\theta}s_{ij} + \frac{\sqrt{3}\sin\theta}{J_2\cos 3\theta}\left\{s_{ip}s_{pj} - \frac{2}{3}J_2\delta_{ij}\right\}\right]\right) \tag{11}$$

where $s_{ij} = \sigma_{ij} - \frac{\sigma_{kk}}{3}$ = the deviatoric stress

$G$ = the elastic shear modulus

$e_{ij} = \varepsilon_{ij} - \frac{\varepsilon_{kk}}{3}$ = the deviatoric strain

$\delta_{ij} = \begin{cases} 1 \text{ for } i = j \\ 0 \text{ for } i \neq j \end{cases}$ = Kronecker delta

$J_2$ and $\theta$ are the second invariant of the deviator stress and the Lode angle, respectively, and will be defined later.

The second term of Equation (11) represents the creep contribution. $F$ is a multiplier on the steady-state creep rate to simulate the transient creep response according to the following equation

$$F = \begin{cases} e^{\Delta[1-\zeta/\varepsilon_t^*]^2}, & \zeta < \varepsilon_t^* \\ 1 & \zeta = \varepsilon_t^* \\ e^{-\delta[1-\zeta/\varepsilon_t^*]^2} & \zeta > \varepsilon_t^* \end{cases} \tag{12}$$

where $\Delta =$ work-hardening parameter

$\delta =$ recovery parameter

$\varepsilon_t^* =$ transient strain limit

$\zeta$ is an internal state variable whose rate of change is determined by the following evolutionary equation

$$\dot{\zeta} = (F - 1)\dot{\varepsilon}_s \tag{13}$$

In Equation (12), the work-hardening parameter $\Delta$ is defined as

$$\Delta = \alpha + \beta \log(\bar{\sigma} / G) \tag{14}$$

where, $\alpha$ and $\beta$ are constants. The variable $\bar{\sigma}$ is the equivalent Tresca stress given by

$$\bar{\sigma} = 2\sqrt{J_2}\cos\theta \tag{15}$$

where $\theta = \frac{1}{3}\arcsin\left[\frac{-3\sqrt{3}J_3}{2(J_2)^{3/2}}\right]$ is the Lode angle limited to the range $(-\frac{\pi}{6} \le \theta \le \frac{\pi}{6})$.

$J_2 = \frac{1}{2}s_{pq}s_{qp}$ = second invariant of the stress deviator

$J_3 = \frac{1}{3}s_{pq}s_{qr}s_{rp}$ = third invariant of the stress deviator

The recovery parameter, $\delta$, is held constant. The transient strain limit is given by

$$\varepsilon_t^* = K_0 e^{cT} (\bar{\sigma} / G)^M \tag{16}$$

where $K_0$, $c$, and $M$ are constants.

The steady-state, or secondary creep strain rate, $\dot{\varepsilon}_s$, is given by

$$\dot{\varepsilon}_s = A_1 e^{-Q_1/R\Theta} \left(\frac{\bar{\sigma}}{G}\right)^{n_1} + A_2 e^{-Q_2/R\Theta} \left(\frac{\bar{\sigma}}{G}\right)^{n_2} + |H| \left[ B_1 e^{-Q_1/R\Theta} + B_2 e^{-Q_2/R\Theta} \right] \sinh \left[ \frac{q(\bar{\sigma} - \sigma_{0)}}{G} \right] \tag{17}$$

Where $A_i$ s and $B_i$ s are constants

$Q_i$ s are activation energies

$\Theta$ = the absolute temperature

$R$ = the universal gas constant

$n_i$ s are the stress exponents

$q$ = the stress constant

$\sigma_0$ = the stress limit of the dislocation slip mechanism

$|H|$ = the Heaviside step function with the argument $(\bar{\sigma} - \sigma_0)$

### *3.1 Input Parameters for the Intact Salt Model*

The material constants used in the analyses for the clean and argillaceous salt are given in Table 2 and Table 3.

Table 2. Salt elastic properties (Butcher 1997)

| Parameter | Value | Units |
|---|---|---|
| *G* | 12,400 | MPa |
| *E* | 31,000 | MPa |
| *ν* | 0.25 | – |

Table 3: Salt creep properties (Munson et al. 1989)

| Parameter | Clean Salt | Argillaceous Salt | Units |
|---|---|---|---|
| $A_1$ | 8.386e+22 | 1.407e+23 | 1/sec |
| $Q_1$ | 25,000 | 25,000 | cal/mole |
| $n_1$ | 5.5 | 5.5 | $n_1$ |
| $B_1$ | 6.086e+06 | 8.998e+06 | 1/sec |
| $A_2$ | 9.672e+12 | 1.314e+13 | 1/sec |
| $Q_2$ | 10,000 | 10,000 | cal/mole |
| $n_2$ | 5.0 | 5.0 | – |
| $B_2$ | 3.034e-02 | 4.289e-02 | 1/sec |
| $\sigma_0$ | 20.57 | 20.57 | MPa |
| $q$ | 5335 | 5335 | – |
| $m$ | 3.0 | 3.0 | – |
| $K_0$ | 6.275e+05 | 2.470e+06 | – |
| $c$ | 9.198e-03 | 9.198e-03 | 1/T |
| $\alpha$ | -17.37 | -14.96 | – |
| $\beta$ | -7.738 | -7.738 | – |
| $\delta$ | 0.58 | 0.58 | – |

## 4 Run Control

Herrick 2012 contains the run control information for the JAS3D analyses in which the emplaced panel closures use a crushed salt fill with initial porosities of 33, 25, 20, and 15% (or initial fractional densities of 67, 75, 80, and 85%, respectively) which were presented in the DOE's response to EPA questions (DOE 2012). This section contains the run control information for the additional analyses in which the emplaced panel closures use crushed salt fill with initial porosities of 35 and 30% (or initial fractional densities of 65 and 70%, respectively). Of perhaps greatest importance is that the results module Jas3d/Output is the same for all analyses including those used in DOE (2012).

For the additional two analyses, JAS3D (version 2.4.C-WIPP) and its associated utilities (Algebra2 (version 1.28), Aprepro (version 2.06), BlotII2_cps (version 1.59A), FASTQ_cps (version 3.18), and GEN3DII (version 1.37a)) were run on April 20, 2012 on seals.sandia.gov using the Python run control scripts PC3R_3.py and PC3R_4.py and the Python module rc.py. The Postscript files generated by BlotII2 (version 1.59A) were converted to PDF files using the UNIX utility ps2pdf. All input files for the runs were exported from the CVS repository $CVSLIB/Analyses/PC3R, module Jas3d/Input/Underground2.

The run control scripts and an associated C shell scripts, RunJas3d_3.csh and RunJas3d_4.csh, were exported from the RunControl module of the same repository. JAS3D and associated utility codes and scripts were exported from code-specific CVS repositories (Table 4). The output files from JAS3D, Algebra, BlotII2, and ps2pdf were stored in the Output module of the repository $CVSLIB/Analyses/PC3R. Additional data files (.dat) produced by BlotII2 were added to the Jas3d/Output module of the repository after the PC3R.py script completed. The log files

PC3R_3.log and PC3R_4.log, and RTF versions of those files, are stored in the module RunControl/Log. All files were tagged with the CVS tag PC3R.

Table 4. Run control code-specific CVS repositories.

| File | Repository | Comment |
|---|---|---|
| Builds/Linux64/algebra2 (Ver:1.28) | /nfs/data/CVSLIB/ACCESS_WIPP/ALGEBRA2 | Manipulates EXODUS finite element output data by evaluating expressions |
| Builds/Linux64/aprepro (Ver:2.06) | /nfs/data/CVSLIB/ACCESS_WIPP/APREPRO | An algebraic preprocessing program |
| Builds/Linux64/blotII2_cps (Ver:1.59A) | /nfs/data/CVSLIB/ACCESS_WIPP/BLOTII2 | Postscript driver for blot |
| Builds/Linux64/fastq_cps (Ver:3.18) | /nfs/data/CVSLIB/ACCESS_WIPP/FASTQ | Finite element 2-dimensional mesh generation program |
| Builds/Linux64/gen3d2 (Ver:1.37a) | /nfs/data/CVSLIB/ACCESS_WIPP/GEN3DII | Transforms a 2-dimensional GENESIS database into a 3-dimensional GENESIS database |
| Builds/Linux64/jas3d (Ver:2.4.C-WIPP) | /nfs/data/CVSLIB/ACCESS_WIPP/JAS3D | Finite element code for 3-dimensional analyses |
| RunControl/algebra2.sh | /nfs/data/CVSLIB/ACCESS_WIPP/ALGEBRA2 | Script for manipulating EXODUS finite element output data by evaluating expressions |
| RunControl/blotII2.sh | /nfs/data/CVSLIB/ACCESS_WIPP/BLOTII2 | Script for running graphics code for examining meshes |
| RunControl/fastq.sh | /nfs/data/CVSLIB/ACCESS_WIPP/FASTQ | Script for running finite element 2-dimensional mesh generation program |
| RunControl/gen3dII.sh | /nfs/data/CVSLIB/ACCESS_WIPP/GEN3DII | Script to transform a 2-dimensional GENESIS database into a 3-dimensional GENESIS database |
| RunControl/jas3d.sh | /nfs/data/CVSLIB/ACCESS_WIPP/JAS3D | Script for running jas3d.exe |

## 5 Results

The following figures, from the PostScript files (Jas3d/Output/*.ps), and associated data files (Jas3d/Output/*.dat), where * indicates the base filename, were used in support of parameter value selections for PCS-2012 PA (Camphouse 2012). Base filenaming for the panel closure analyses takes one of two forms: “pclo_vcXX_por-void” or “pclo_vcXX_SIG-DY”. Here “plco” signifies that the analyses were of panel closures with the underground stratigraphy included, “vcXX” indicates that the model used for the run-of-mine salt was the volumetric creep model beginning with an initial fractional density of XX percent, “por-void” means that the analyses considered porosity and void volume properties of the crushed salt, and “SIG-DY” means that the analyses looked at stresses and vertical displacements of the back of the drift or top of the crushed salt. For the latest two analyses, the filename “vc65” indicates that the run-of-mine salt was modeled with the volumetric creep model having an initial fractional density of 65%, and filename “vc70” indicates that the run-of-mine salt was modeled as having an initial fractional density of 70%. The same filenaming convention is used for the previous set of analyses where the initial fractional densities 67, 75, 80, and 85% (Herrick 2012).

### *5.1 Porosity History Plots*

Starting with the smallest initial density (fractional density = 65%) and progressing to the highest (fractional density = 85%), the porosity histories through the first 500 years for all JAS3D underground analyses are given in Figure 2 through Figure 7.

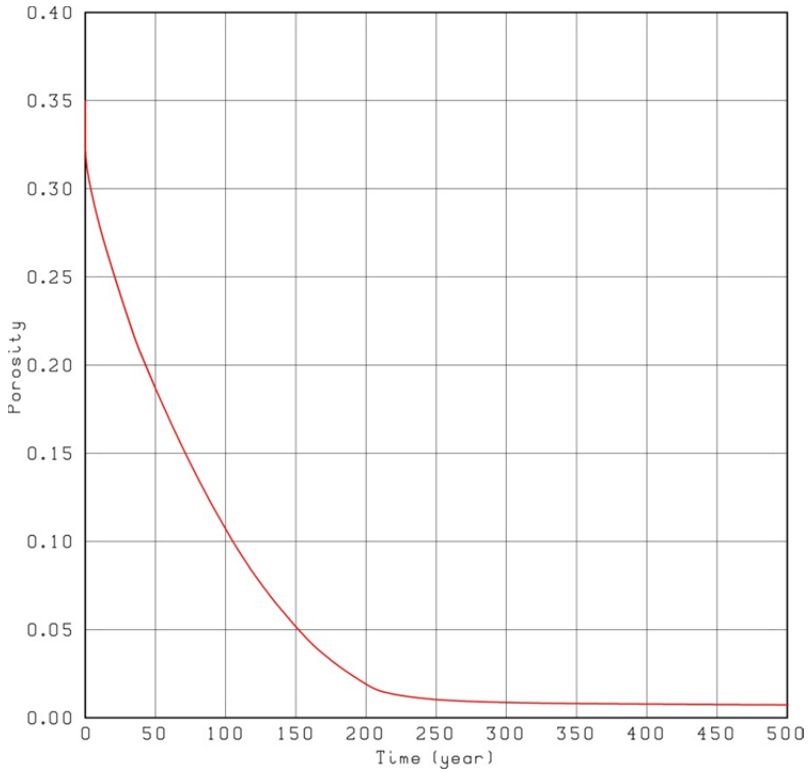


Figure 2. Porosity history through 500 years for a crushed salt panel closure in the intake drift having an initial porosity of 35%, which corresponds to an initial fractional density of 65%.

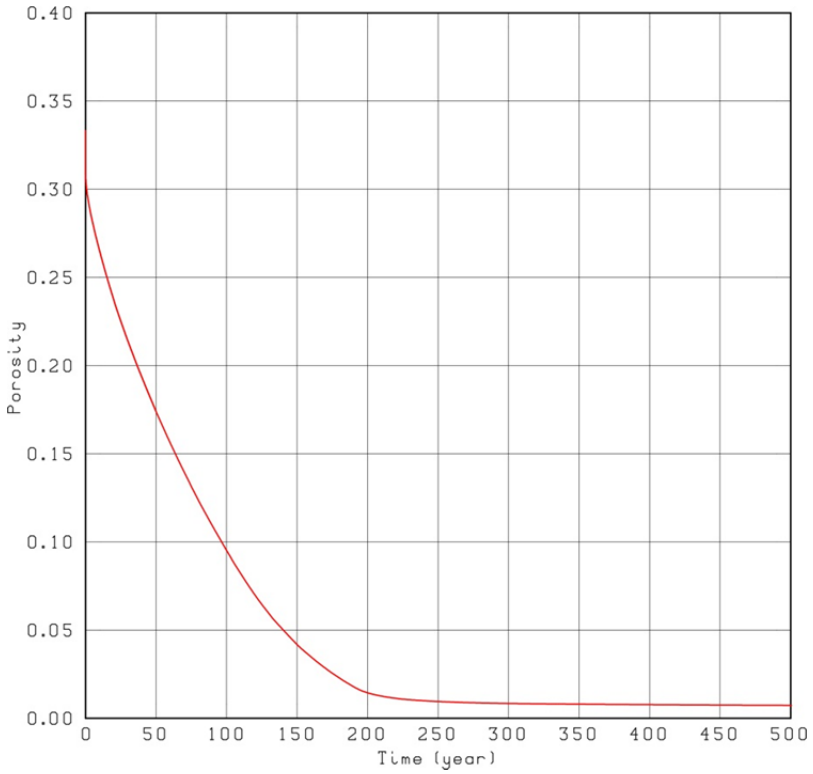


Figure 3. Porosity history through 500 years for a crushed salt panel closure in the intake drift having an initial porosity of 33%, which corresponds to an initial fractional density of 67%.

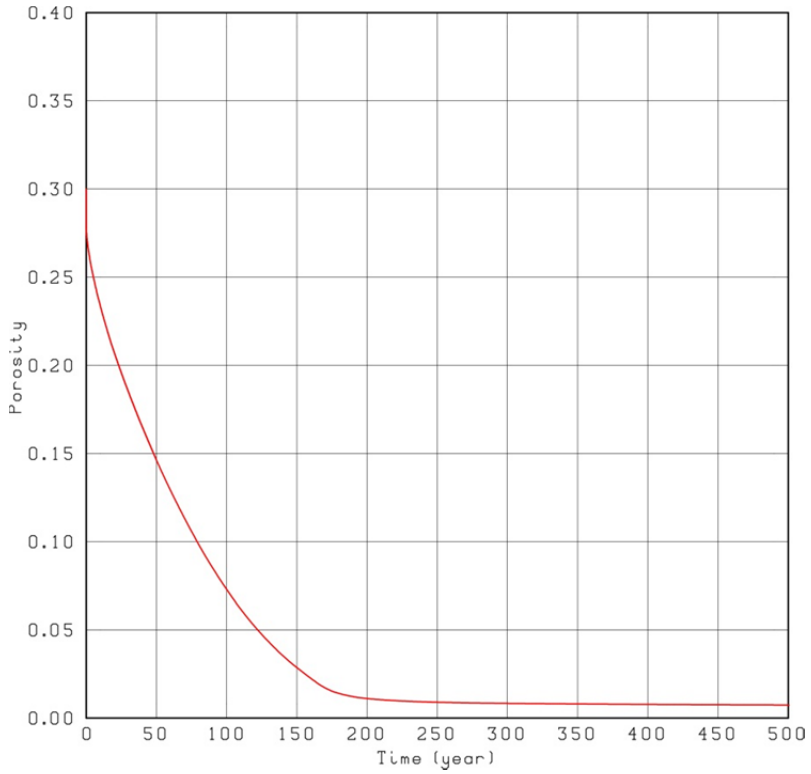


Figure 4. Porosity history through 500 years for a crushed salt panel closure in the intake drift having an initial porosity of 30%, which corresponds to an initial fractional density of 70%.

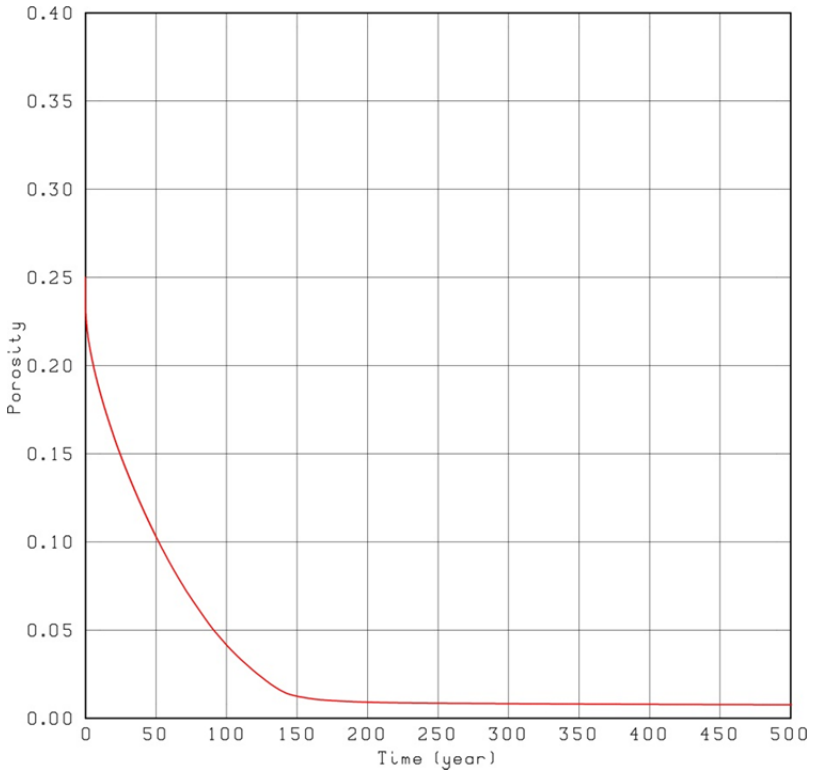


Figure 5. Porosity history through 500 years for a crushed salt panel closure in the intake drift having an initial porosity of 25%, which corresponds to an initial fractional density of 75%.

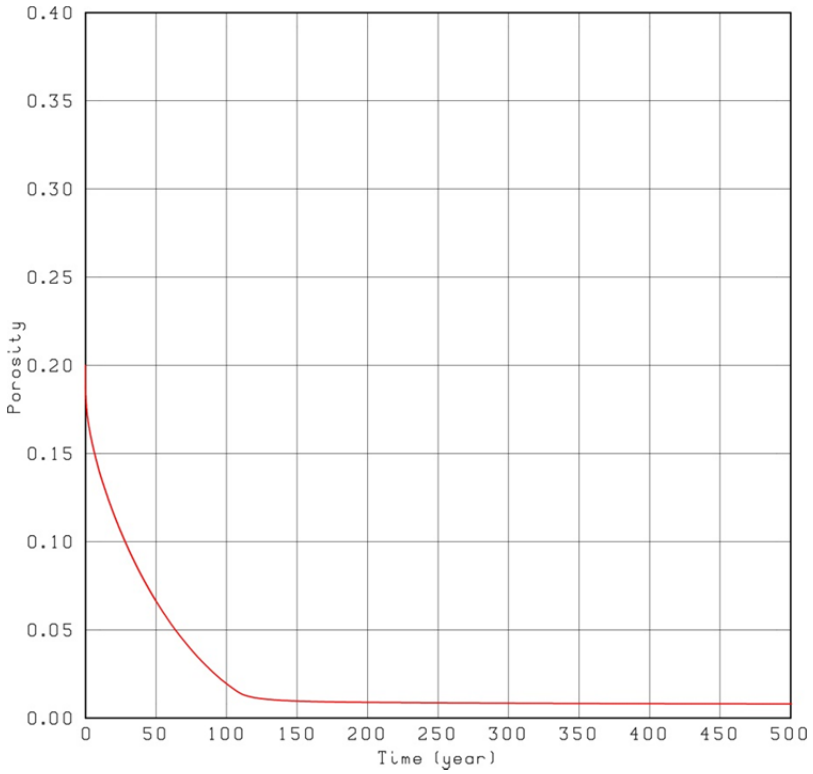


Figure 6. Porosity history through 500 years for a crushed salt panel closure in the intake drift having an initial porosity of 20%, which corresponds to an initial fractional density of 80%.

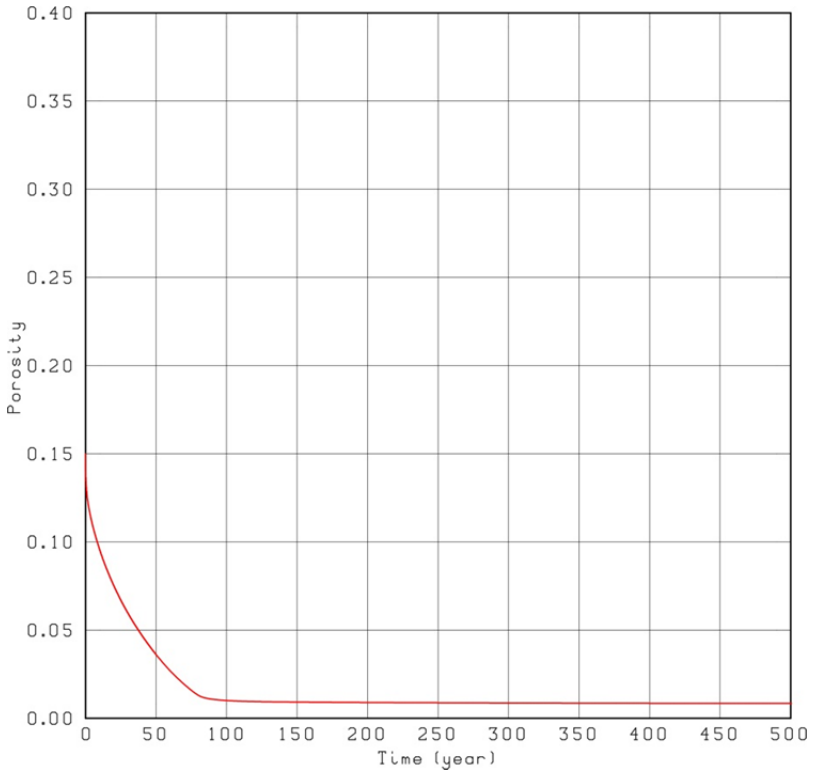


Figure 7. Porosity history through 500 years for a crushed salt panel closure in the intake drift having an initial porosity of 15%, which corresponds to an initial fractional density of 85%.

As a check of the consistency of the results obtained from JAS3D by the method described herein, a plot of the time at which the crushed salt in the panel closure consolidates to a porosity of 5% for the six different initial porosities is shown in Figure 8. The high $R^2$ value demonstrates the consistency of the analytical method. The relationship was fit by a linear trend line using Excel.

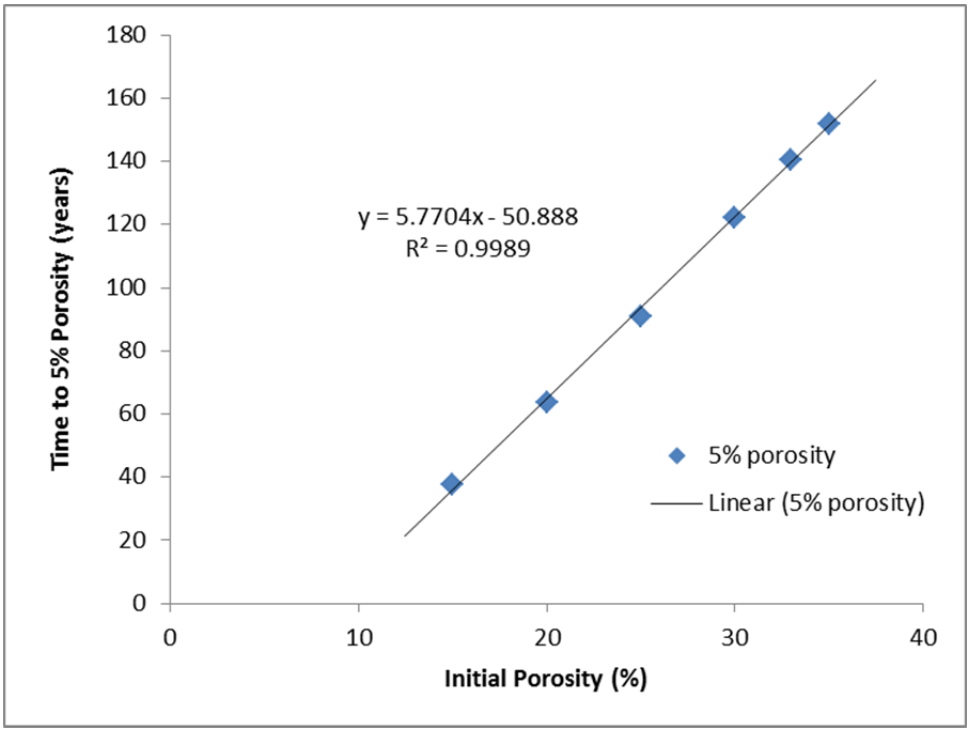


Figure 8. Plot of the time it takes for the crushed salt fill in the panel closures to reach 5% porosity starting from the six different initial porosities used in the JAS3D analyses.

### *5.2 Backstress in the Back (Roof) of the Drift History Plots*

The backstresses generated by the crushed salt in the back (roof) of the intake drift resulting from consolidation of the crushed salt filling a panel closure was estimated graphically. The next series of plots, Figure 9 through Figure 14, are histories of the vertical stress in the back of the drift again through the first 500 years. The location of the element used to obtain the data is in the center of the drift.

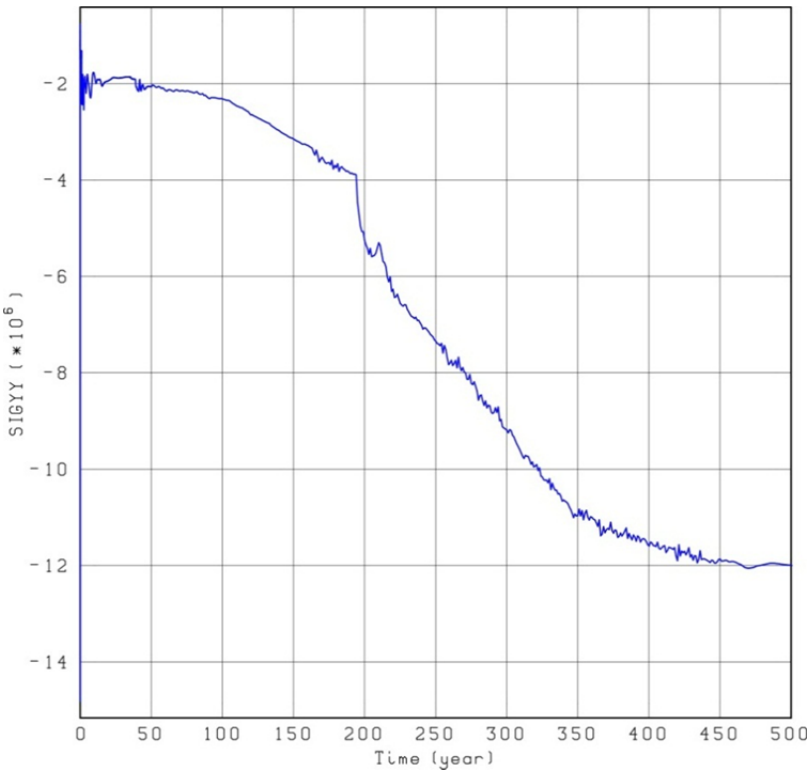


Figure 9. Vertical stress history through 500 years in the back (roof) of the intake drift produced by a run-of-mine salt panel closure having an initial porosity of 35%.

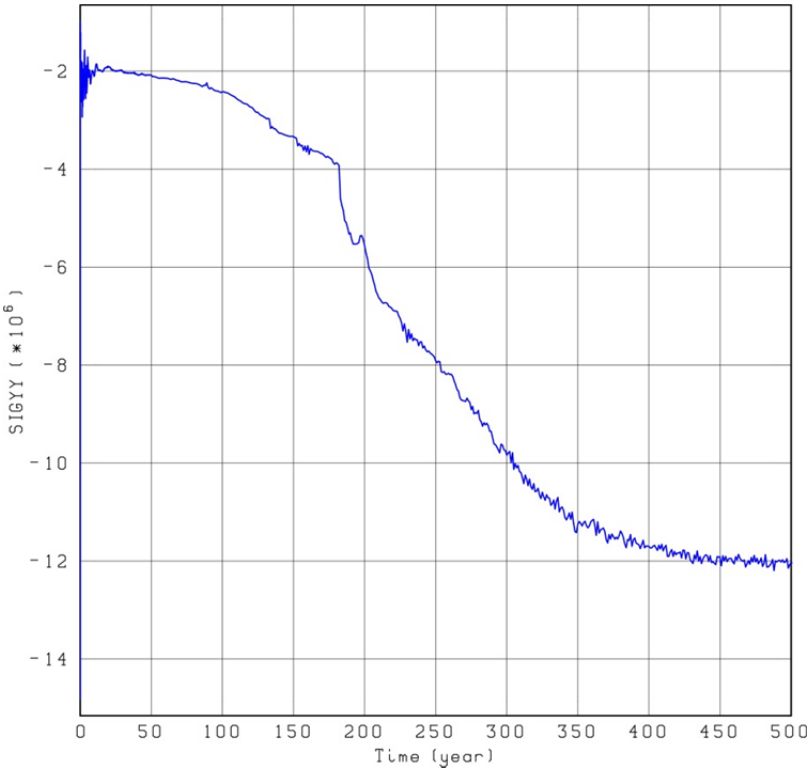


Figure 10. Vertical stress history through 500 years in the back (roof) of the intake drift produced by a run-of-mine salt panel closure having an initial porosity of 33%.

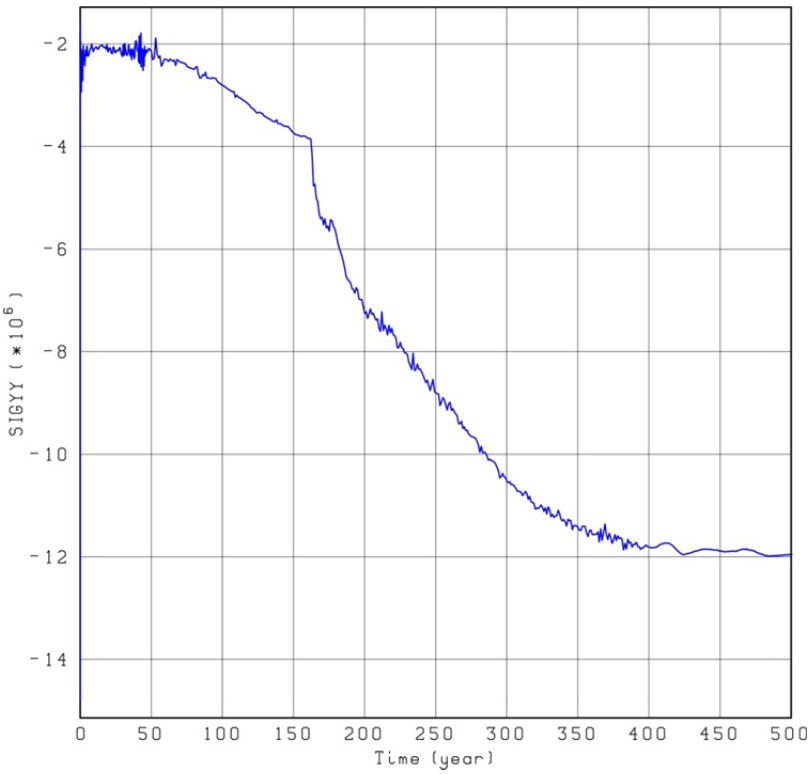


Figure 11. Vertical stress history through 500 years in the back (roof) of the intake drift produced by a run-of-mine salt panel closure having an initial porosity of 30%.

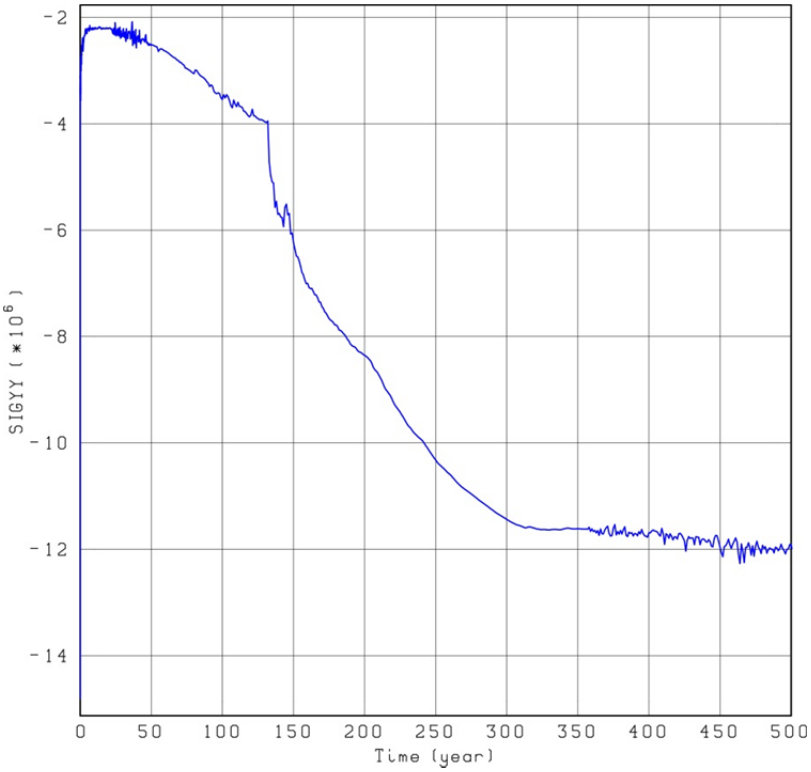


Figure 12. Vertical stress history through 500 years in the back (roof) of the intake drift produced by a run-of-mine salt panel closure having an initial porosity of 25%.

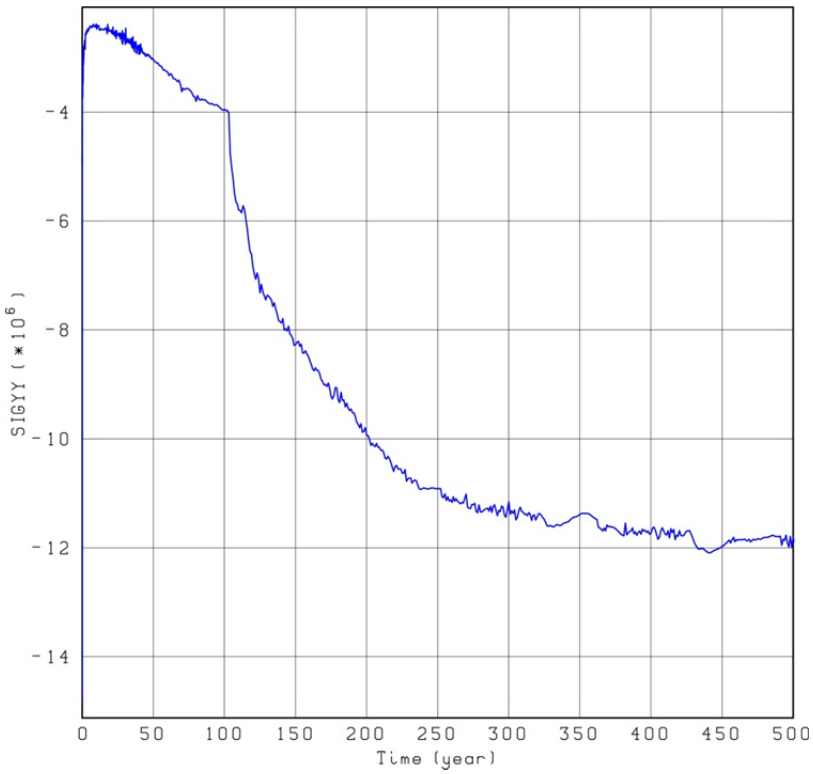


Figure 13. Vertical stress history through 500 years in the back (roof) of the intake drift produced by a run-of-mine salt panel closure having an initial porosity of 20%.

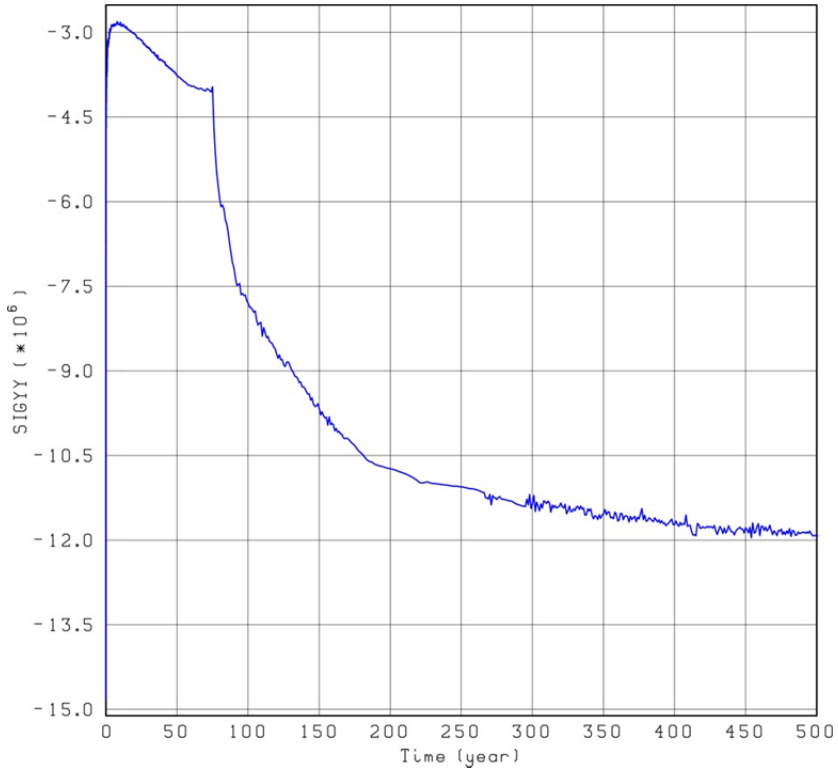


Figure 14. Vertical stress history through 500 years in the back (roof) of the intake drift produced by a run-of-mine salt panel closure having an initial porosity of 15%.

## 6 References:


Brodsky, N.S. 1994. Determination of the Intact Density of WIPP Salt Specimens. Calculation No. 325/03/02. Respec Inc., Rapid City, SD

Butcher, B.M. 1997. A Summary of the Sources of Input Parameter Values for the WIPP Final Porosity Surface Calculations. SAND97-0796. Sandia National Laboratories, Albuquerque, NM

Camphouse, R.C., M. Gross, C.G. Herrick, D.C. Kicker, B. Thompson. 2012. Recommendations and Justifications of Parameter Values for the Run-of-Mine Salt Panel Closure System Design Modeled in the PCS-2012 PA. Sandia National Laboratories, Carlsbad, NM

DOE (U.S. Department of Energy). 2012. Response to First Set of EPA Questions to DOE, December 22, 2011. Letter from Mr. Juan Franco, Manager, Carlsbad Area Field Office, U.S. Department of Energy, to Mr. Jonathan Edwards, Director, Radiation Protection Division, U.S. Environmental Protection Agency, dated April 17, 2012.

Herrick, C.G. 2012. Calculations Performed in Support of Reconsolidation of Crushed Salt in Panel Closures. Memorandum to the WIPP Records Center dated March 29, 2012. ERMS 557150. Sandia National Laboratories, Carlsbad, NM.

Holcomb, D.J. and M.F. Shields. 1987. Hydrostatic Consolidation of Crushed Salt with Added Water. SAND87-1990., Sandia National Laboratories, Albuquerque, NM

Itasca Consulting Group. 2003. FLAC3D: Fast Lagrangian Analysis of Continua in 3 Dimensions User's Guide. Version 2.1, Optional Features, Section 2 – Creep Materials Models. Minneapolis, MN

Krieg, R. D. 1984. Reference Stratigraphy and Rock Properties for the Waste Isolation Pilot Plant (WIPP) Project. SAND83-1908. Sandia National Laboratories, Albuquerque, NM

Munson, D.E. and P.R. Dawson. 1979. Constitutive Model for the Low Temperature Creep of Salt (with Application to WIPP). SAND79-1853. Sandia National Laboratories, Albuquerque, NM

Munson, D.E. and P.R. Dawson. 1982, A Transient Creep Model for Salt during Stress Loading and Unloading. SAND82-0962. Sandia National Laboratories, Albuquerque, NM

Munson, D.E. and P.R. Dawson. 1984. Salt Constitutive Modeling Using Mechanism Maps. The Mechanical Behavior of Salt, Proceedings of the First Conference. Pennsylvania State University, University Park, PA. November 9-11, 1981. H.R. Hardy, Jr. and M. Langer, eds. Karl Distributors, Rockport, MA. pp. 717-737.

Munson, D.E., A.F. Fossum, and P.E. Senseny. 1989. Advances in Resolution of Discrepancies between Predicted and Measured in Situ Room Closures. SAND88-2948. Sandia National Laboratories, Albuquerque, NM

Park, B.Y. and J.F. Holland. 2007. Structural Evaluation of WIPP Disposal Room Raised to Clay Seam G. SAND2007-3334. Sandia National Laboratories, Albuquerque, NM

Sjaardema, G.D. and R.D. Krieg. 1987. A Constitutive Model for the Consolidation of WIPP Crushed Salt and Its Use in Analyses of Backfilled Shafts and Drift Configurations. SAND87-1977. Sandia National Laboratories, Albuquerque, NM

Stone, C.M. 1997a. SANTOS – A Two-Dimensional Finite Element Program for the Quasistatic, Large Deformation, Inelastic Response of Solids. SAND90-0543. Sandia National Laboratories, Albuquerque, NM

Stone, C.M. 1997b. Final Disposal Room Structural Response Calculations. SAND97-0795. Sandia National Laboratories, Albuquerque, NM

WIPP PA. 2009. Verification and Validation Plan / Validation Document for JAS3D Version 2.4.C-WIPP, document version 2.4.C-WIPP. ERMS 545606. Sandia National Laboratories, Carlsbad, NM.